Acute Acidification of Stratum Corneum Membrane Domains Using Polyhydroxyl Acids Improves Lipid Processing and Inhibits Degradation of Corneodesmosomes

Jean-Pierre Hachem[1], **Truus Roelandt**[1], **Nanna Schürer**[2], **Xu Pu**[3], **Joachim Fluhr**[4], **Christina Giddelo**[1], **Mao-Qiang Man**[3], **Debra Crumrine**[3], **Diane Roseeuw**[1], **Kenneth R. Feingold**[3], **Theodora Mauro**[3], and **Peter M. Elias**[3]

[1]Department of Dermatology, Universitair Ziekenhuis Brussel-Vrije Universiteit Brussel, Brussels, Belgium

[2]Department of Dermatology, University of Osnabruck, Osnabruck, Germany

[3]Departments of Dermatology and Metabolism, University of California San Francisco, Veterans Affairs Medical Center, San Francisco, California, USA

[4]Bioskin GmbH, Berlin, Germany

Abstract

Neutralization of the normally acidic stratum corneum (SC) has deleterious consequences for permeability barrier homeostasis and SC integrity/cohesion attributable to serine proteases (SPs) activation leading to deactivation/degradation of lipid-processing enzymes and corneodesmosomes (CD). As an elevated pH compromises SC structure and function, we asked here whether SC hyperacidification would improve the structure and function. We lowered the pH of mouse SC using two polyhydroxyl acids (PHA), lactobionic acid (LBA), or gluconolactone (GL). Applications of the PHA reduced the pH at all levels of SC of hairless mouse, with further selective acidification of SC membrane domains, as shown by fluorescence lifetime imaging. Hyperacidification improved permeability barrier homeostasis, attributable to increased activities of two key membrane-localized, ceramide-generating hydrolytic enzymes (β-glucocerebrosidase and acidic sphingomyelinase), which correlated with accelerated extracellular maturation of SC lamellar membranes. Hyperacidification generated "supernormal" SC integrity/cohesion, attributable to an SP-dependent decreased degradation of desmoglein-1 (DSG1) and the induction of DSG3 expression in lower SC. As SC hyperacidification improves the structure and function, even of normal epidermis, these studies lay the groundwork for an assessment of the potential utility of SC acidification as a therapeutic strategy for inflammatory dermatoses, characterized by abnormalities in barrier function, cohesion, and surface pH.

Introduction

The stratum corneum (SC) of mammalian skin normally shows markedly acidic pH (Schade and Marchionini, 1928; Ohman and Vahlquist, 1994), and its origins and importance are now

Conflict of Interest: The authors state no conflict of interest.

being clarified (Hachem *et al.*, 2003). This so-called "acid mantle" originates at least in part from two endogenous mechanisms that are operative in the outer epidermis, that is, from the secretory phospholipase A_2 (sPLA$_2$)-mediated, extracellular generation of free fatty acids (FFA) from phospholipids (Fluhr *et al.*, 2001), and from the activity of a sodium–proton exchanger, type 1 (NHE1) (Behne *et al.*, 2002), which localizes to the membrane domains of the outer granular layer (Behne *et al.*, 2002; Hachem *et al.*, 2005a). Evidence is accumulating that a third outer epidermal mechanism, that is, generation of trans-urocanic acid from filaggrin proteolysis (Krien and Kermici, 2000), could also be important, as SC pH is elevated in filaggrin-deficient patients with ichthyosis vulgaris (Ohman and Vahlquist, 1998).

Initially linked to antimicrobial function (Korting *et al.*, 1987), the acidic pH of the SC also regulates at least two other epidermal functions, that is, permeability barrier homeostasis and SC integrity/cohesion (the converse of desquamation). For example, barrier recovery is delayed when acutely perturbed skin sites are exposed to a neutral pH buffer (Mauro *et al.*, 1998), and either pharmacological blockade or knockout of sPLA$_2$ or the NHE1 transporter alters permeability barrier homeostasis and SC integrity/cohesion (Fluhr *et al.*, 2001; Behne *et al.*, 2002). Moreover, neutralization of murine SC with topical, non-toxic "superbases" also negatively affects both permeability barrier homeostasis and SC integrity and cohesion (Hachem *et al.*, 2003, 2005b). Furthermore, the abnormalities in the permeability barrier function and SC integrity, characteristic of neonatal skin, are linked to developmental alterations in endogenous acidification, attributable in turn to reduced sPLA$_2$ activity (Fluhr *et al.*, 2004a, 2004b). The negative consequences of SC neutralization have been further linked to the activation of serine proteases (SPs), which display neutral-to-alkaline pH optima (Brattsand *et al.*, 2005). When the pH-induced increase in SP activity is sustained, key lipid-processing enzymes (β-glucocerebrosidase (β-GlcCer'ase) and acidic sphingomyelinase (aSMase)) and corneodesmosome (CD)-constituent proteins are degraded (Fluhr *et al.*, 2004b; Hachem *et al.*, 2005b). Inhibition of lamellar body (LB) secretion comprises yet another recently described negative consequence of pH-induced SP activation, signaled by the protease-activated receptor-2 (Hachem *et al.*, 2006a). Finally, SP activation within SC converts pro-IL-1β to active metabolites, which could initiate inflammation if enzyme activity is sustained (Nylander-Lundqvist and Egelrud, 1997).

As most inflammatory dermatoses show not only primary cytokine activation but also prominent abnormalities in epidermal function, including impaired permeability barrier homeostasis, abnormal desquamation, often increased colonization by pathogenic microbes, pH-driven changes in SP, and lipid-processing enzyme activity, could occur that are clinically relevant. Moreover, not only inflamed skin but also, as noted above, both neonatal and aged skin show a neutral SC pH (Thune *et al.*, 1988; Giusti *et al.*, 2001; Bernard *et al.*, 2003), with known deleterious consequences (Giusti *et al.*, 2001; Choi *et al.*, 2007). Furthermore, the notorious irritation of skin, produced by alkaline soaps, could reflect SP-mediated activation of primary cytokines. Thus, reversal of the pH abnormality in these inflammatory dermatoses might not only improve the permeability barrier function but it also could reduce excess scale, decrease pathogen colonization, and restrict inflammation. To assess the potential utility of hyperacidification as a therapeutic/preventive strategy, we first assessed here its effects on function in normal hairless mouse skin. Our results show first that SC hyperacidification further improves epidermal structure and function, even in normal skin, and second, that the basis for improved function is selective acidification of membrane domains in the lower SC.

Results

PHA decrease pH throughout SC and selectively within membrane microdomains

To assess the effects of polyhydroxyl acid (PHA) applications on the pH of murine SC, we applied either lactobionic acid (LBA) or gluconolactone (GL) (10% in propylene glycol/

ethanol; PG/E: 70:30) once to hairless mice flanks, followed by the measurement of surface pH with a flat surface electrode. A single application of either LBA or GL significantly lowered the surface pH of SC in comparison-neutralized LBA (nLBA in PG/E), GL (nGL in PG/E), or vehicle (PG/E) alone (Figure 1a and b), with gradual recovery toward basal (pretreatment) pH values over the subsequent 24–36 hours after PHA applications (Figures 1b and 2b). Neither the PHA- nor the acidic buffer-treated sites displayed evidence of irritation, assessed grossly as visible inflammation, histologically as absence of both epidermal hyperplasia and dermal inflammation, and biophysically as an absence of changes in transepidermal water loss (TEWL) levels (data not shown).

To ascertain the localization of the PHA-induced pH changes within SC, we next assessed pH at different levels of SC of hairless mouse. As shown both by sequential tape stripping and by fluorescence lifetime imaging microscopy (FLIM) (see below), the LBA-induced decrease in pH at 3 hours extended to all levels of murine SC (4–5 strippings, remove all layers of stratum disjunction in normal hairless mice) (Figure 1c).

The acidic pH of normal mouse SC is inhomogeneously distributed—although pH is lower in the outer than in the lower SC (Ohman and Vahlquist, 1994), membrane domains remain acidic even in the lower SC, extending to the stratum granulosum (SG)–SC interface (Behne *et al.*, 2002; Hanson *et al.*, 2002). To ascertain which levels and subcellular sites of SC are acidified by the PHA, we next used FLIM to assess the microdomain distribution of pH 1–3 hours after twice-daily applications of either LBA or nLBA to hairless mouse skin. The pH-sensitive fluorophore, 2, 7-bis-(2-carboxyethyl)-5-(and -6)-carboxyfluorescein (BCECF), was applied topically shortly before biopsy, followed by the *ex vivo* examination of samples in the confocal/FLIM microscope. pH of membrane (extracellular) domains and intracellular (cytosolic) domains was comparable in nLBA-treated skin (Figures 1d and 2). In contrast, LBA treatment decreased pH at all levels of murine SC, with a further reduction in membrane microdomains in the lower SC (by about 1 pH unit), extending downward to the SG–SC interface (Figures 1d and 2). Yet the pH of the underlying nucleated layers did not appear to change (Figure 2). Together, these studies show that (1) topical PHA applications hyperacidify both the cytosolic and membrane compartments of all levels of SC; (2) hyperacidification is restricted to SC; and (3) hyperacidification further reduces pH in SC membrane domains.

Hyperacidification of acutely disrupted skin accelerates barrier recovery attributable to enhanced lipid processing

To determine whether hyperacidification improves permeability barrier function in murine epidermis, we next assessed barrier recovery kinetics following acute abrogation by tape stripping after applications of PHA (as above). Both LBA and GL were applied immediately after tape stripping (TEWL ≥ 10 mg cm^{-2} hour^{-1}) to opposing flanks of hairless mice, and TEWL was assessed 3 hours later. Barrier recovery kinetics accelerated significantly in sites that were acidified with either LBA or GL in comparison with neutralized PHA (nPHA) or vehicle-treated sites (Figure 3). As recovery rates were comparable in neutralized PHA and vehicle-treated sites, the PHA molecule alone does not appear to influence permeability barrier homeostasis.

To assess the structural basis for accelerated recovery, we next compared the LB secretory system 3 hours after either PHA or neutralized PHA applications to hairless mice. Electron micrographs showed no differences in either the cytosolic density (no. of) or the extent of secretion of LB in PHA-treated vs control sites (data not shown). Instead, the rate of formation of mature lamellar membranes appeared to be accelerated in LBA-treated sites; that is, large numbers of mature bilayers appeared within the SG–SC interface of PHA-treated skin sites (Figure 4a, right panel, arrows), whereas control sites showed fewer mature membranes at this

level These ultrastructural observations suggest that PHA treatment accelerates the transformation of secreted LB contents into "mature" lamellar bilayers.

To assess the biochemical basis for the PHA-induced acceleration of barrier recovery and membrane maturation, we next assessed changes in the activities of the two key lipid-processing enzymes that show acidic pH optima, β-GlcCer'ase and aSMase. By *in situ* zymography, the activities of both β-GlcCer'ase and aSMase increased in the lower SC after hyperacidification with either of the PHA after acute barrier disruption (Figure 4b; GL results not shown). The acidification-induced increases in enzyme activity in murine epidermis were abolished when frozen sections of hyperacidified skin were buffered to a neutral pH (Figure 4b; *in situ* neutralized). Together, these results show that hyperacidification accelerates barrier recovery by stimulating the maturation of extracellular lamellar membranes, which in turn is attributable to the enhanced activities of key lipid-processing enzymes with acidic pH optima.

Hyperacidification improves SC integrity and reduces desquamation rates attributable to a decrease in bulk SP activity and induction of DSG3 expression

To assess the potential beneficial effects of hyperacidification for SC integrity/desquamation, we next assessed SC integrity after the application of LBA and GL to normal hairless mouse skin, as above. Both of the PHA significantly improved SC integrity in normal murine SC, a change that became particularly evident deep in the SC (Figure 5a; note significant differences in TEWL after both third and fourth strippings). SC cohesion (amount of protein per stripping) also improved significantly in the lower SC of PHA-treated murine skin, shown as less protein removed per stripping (Figure 5b). These results show that hyperacidification improves SC integrity and cohesion in normal murine skin.

We next assessed the basis for improved SC integrity in PHA-treated hairless mouse skin. Although CD degradation normally begins 1–2 layers above the SG–SC interface, CD instead persisted to the mid-to-outer SC in LBA-treated sites (Figure 6a and b). These differences were confirmed further by quantitative electron microscopy in randomized, coded micrographs that showed a significant increase in CD density in the lower SC in hyperacidified SC (Figure 6b). We next assessed whether the LBA-induced increase in CD density was attributable to retention of intact, constituent CD proteins, assessed as the desmoglein-1 (DSG1) content in western blots of SC extract from LBA and vehicle-treated murine SC. To differentially address the effect of acidification of the different layers of the SC, we removed the SC by applying four sequential D-squames on the same area of the flanks to a total of four areas per animal. The first two D-squames were considered as upper SC and were extracted separately from the third and fourth D-squames, which were regarded as lower SC. Thus, a comparison by western immunoblotting was carried out between the lower and upper SC from both hyperacidified and control-treated mice. When compared with vehicle, western immunoblotting indicated a decreased proteolysis of DSG1 in hyperacidified upper SC (Figure 6c). Surprisingly, DSG1 protein was significantly decreased in hyperacidified lower SC compared with vehicle l (Figure 6c). However, DSG3, which is normally absent in the SC, was increased in the protein fraction of the lower SC treated with LBA (Figure 6c). The 3-hour time period between tape stripping and sample collection should suffice for newly synthesized DSG3, as new corneocytes are formed within 20 minutes after tape stripping (Demerjian *et al.*, 2008). Also, we have found that either neutralizing or acidifying the SC increases or decreases sodium hydroxide anti-porter (NHE-1) *in vivo* in a time frame of 3 hours (Hachem *et al.*, 2005a). These results show that the hyperacidification of murine SC leads to persistence of CD, by the decreased degradation of DSG1 in the upper levels of the SC and the induction of DSG3 expression in the lower parts of the SC, providing a structural basis for the improved SC integrity/cohesion of hyperacidified normal skin.

Although SP activity is quite low in SC of normal hairless mouse under basal conditions, SP activity became virtually undetectable in hyperacidified murine SC (Figure 7a). These changes reflect a pH-induced inhibition in enzyme activity alone, because neutralization of previously acidified frozen tissue sections restored, or even increased, enzyme activity (Figure 7a; *in situ* neutralization). Moreover, a complementary method to assess SP activity, the soybean trypsin inhibitor (STI) binding assay, also showed less binding of the SP inhibitor to hyperacidified SC, which is also indicative of lower SP activity in PHA-treated skin (Figure 7b). In addition, western immunoblotting for both kallikrein (klk) 5 and 7, the two SPs most clearly linked to SC desquamation, showed decreased immunostaining for the proteolytically active forms at 28 and 31 kDa, respectively (Figure 7d), suggesting that hyperacidification decreases not only SP activity but also the levels of proteolytically active protein. Finally, both pro-klk5 and pro-klk7 are restricted to lipid raft (LR) domains in hyperacidified SC, whereas both active forms of the two SPs became non-LR bound in control samples (Figure 7d). Together, these results show that the hyperacidification of SC reduces the activity, active protein content, and localization of SP.

In addition to SP, the SC also contains both aspartate and cysteine proteases that show acidic pH optima (e.g., cathepsins D, E and L2), which have a potential role in desquamation (Behrendt and Green, 1958; Igarashi *et al.*, 2004) and permeability barrier homeostasis (Egberts *et al.*, 2004). To ascertain whether SC hyperacidification also affects cathepsin activity, we next carried out an *in situ* pepstatin A binding assay on murine skin sites, treated earlier with LBA. Unlike the application of control after tape stripping, the apparent levels of pepstatin A binding to SC was similar in LBA and nLBA skin sites (Figure 7c), suggesting that SC acidification alone did not suffice to increase enzyme activity, whereas barrier status (nLBA + TS) increases cathepsin D activity as suggested earlier by Egberts *et al.* (2004). In addition, only pro-cathepsin D (52 kDa) was observed within the non-LR domains on western immunoblotting from the epidermal extracts of both LBA- and nLBA-treated SC (Figure 7d), further suggesting that cathepsin D activation does not change with hyperacidification. Together, these results show that the improved SC integrity/cohesion of hyperacidified SC is due to CD retention, attributable to a further reduction in SP activity within treated SC.

Discussion

In normal mammals, acute perturbations of the permeability barrier elicit metabolic responses in the underlying epidermis that rapidly restore barrier homeostasis. These responses include the rapid secretion of a preformed pool of LBs (Menon *et al.*, 1985, 1992) and the stimulation of lipid synthesis (Menon *et al.*, 1985; Grubauer *et al.*, 1989). This initial cascade leads to partial barrier restoration, with the final stages of barrier repair resulting sequentially from (1) an upregulation of epidermal ceramide synthesis (Holleran *et al.*, 1991); (2) increased production of lipid-processing enzymes (Holleran *et al.*, 1992), such as β-GlcCer'ase (Holleran *et al.*, 1994); and (3) increased epidermal DNA synthesis (Proksch *et al.*, 1991). Normalization of barrier function is largely completed by 35 hours in mice (Menon *et al.*, 1985; Grubauer *et al.*, 1989). Given the rapidity of the amplified response to acute barrier disruption in normal epidermis, it is remarkable that a further decrease in the pH of normal SC significantly accelerates the timetable of barrier recovery in both humans and mice. Also of interest is the apparent lack of toxicity of PHA applications to mouse skin, reflecting the localization of metabolic effects to the SC alone, as shown by FLIM analysis.

The improved function of hyperacidified SC could be attributed not only to a broad reduction in SC pH but also to a still further reduction of pH within SC membrane domains. The decline in pH (from 5.5–6 to levels of ≤5) further optimizes the activities of two key lipid-processing enzymes, β-GlcCer'ase and aSMase, which both display optimum activities at ≈ pH ≤5.0 (Vaccaro *et al.*, 1985; Takagi *et al.*, 1999), and which further localize to membrane domains

of the SC (these studies; Vaccaro *et al.*, 1985; Hachem *et al.*, 2003; Igarashi *et al.*, 2004). The pH-induced boost in lipid-processing enzymes, in turn, appears to accelerate the rate of maturation of secreted LB contents into broad lamellar membranes. Thus, improved lipid processing accounts, at least in part, for the hyperacidification-induced improvement in permeability barrier homeostasis. Hyperacidification could also improve barrier function by a second mechanism, that is, a pH-induced decline in SP activity (Hachem *et al.*, 2006a), that could accelerate LB secretion (Denda *et al.*, 1997), in a protease-activated receptor-2-dependent manner (Hachem *et al.*, 2006a), but this mechanism was not assessed in these studies.

The decline in pH also improves SC integrity and cohesion (decreasing desquamation rates), because of a further reduction in the already low basal SP activity to levels that became almost undetectable. The further decline in SP activity is consistent with the neutral-to-alkaline pH optima of SP in general and of klk5 and klk7 specifically (Brattsand *et al.*, 2005). Although the epidermis contains a broad panoply of klks, these two SP, and the recently described klk8 (Kishibe *et al.*, 2007), appear to be the dominant, desquamatory SP of the SC (Caubet *et al.*, 2004; Brattsand *et al.*, 2005). As SP activity reverts to basal or supernormal levels when previously acidified SC is neutralized, a pH-induced decrease in enzyme protein levels likely does not account for the hyperacidification-induced decline in SP activity, a conclusion supported by western blot quantitation of these proteins. These observed shifts in enzyme activity have important structural consequences that explain the apparent benefits of hyperacidification for desquamation. Similarly, Fartasch *et al.* (1997) showed that 3 weeks of treatment with a 4% glycolic enhanced desmosomal breakdown only within the stratum disjunctum, whereas desmosomes of the stratum compactum were unaffected and appeared more compacted (Fartasch *et al.*, 1997). Moreover, Kim *et al.* (2001) applied both glycolic and lactic acid at 5% for 14 days on hairless mouse flanks and showed a reduction in SC thickness on the sites of acid application (Kim *et al.*, 2001).

In our studies, we used a single application of PHA on either intact or tape-stripped SC to assess the integrity and permeability barrier function of SC. We showed that the reduction in SP activity correlated with increased CD density in the deeper layers of hyperacidified SC, explaining the improved SC integrity and cohesion at this level and the compacted appearance of the SC at deeper levels. Yet decreased SP activity alone cannot explain the improved integrity and the increase in CD density. We also observed that SC hyperacidification induces the expression of DSG3, which is normally absent from the SC. Although our zymographic data clearly show a decrease in SP activity, both klk5 and 7 could still retain some activity, even at lower pH levels (Caubet *et al.*, 2004). The observed increase in LB secretion reported by Kim *et al.* (2001) could either be related to a reduction in SP activity and protease-activated receptor-2 signaling of LB secretion (Hachem *et al.*, 2006a) or it could reflect increased epidermal proliferation, a well-known consequence of topical alpha-hydroxyl acid applications (Ditre *et al.*, 1996). The SC pH gradient allows the precise regulation of klk5 activity by controlling the interaction of this SP with the SP inhibitor, LEKTI, leading to the release of active klk from LEKTI–klk complexes at an acidic pH and klk-mediated corneodesmosomal cleavage in the superficial layers of the SC (Deraison *et al.*, 2007). We propose, therefore, that SC acidification allows the dissociation of LEKTI–klk complexes, inhibiting DSG1 degradation in lower SC. Klk5 still possesses a proteolytic activity profile at pH 5.6 (Caubet *et al.*, 2004), activating the klk cascade and allowing degradation of CDs (Caubet *et al.*, 2004; Emami and Diamandis, 2008). Mutations of LEKTI in the Netherton syndrome cause unrestricted activation of SP, resulting in DSG1 breakdown, also accompanied by a compensatory expression of DSG3 (Hachem *et al.*, 2006b), as observed here. Thus, the improved integrity and cohesion of the SC from PHA treatment can likely be attributed to both a decrease in bulk SC protease activity leading to DSG1 persistence and the induction of DSG3 in the lower SC.

As cysteine and aspartate proteases, two protease families with acidic pH optima (i.e., cathepsin D, E, L2), are also present in the SC (Bernard *et al.*, 2003; Igarashi *et al.*, 2004), it is possible that hyperacidification of SC could accelerate desquamation, based on increased cathepsin activity. Yet hyperacidification alone under these conditions did not appear to increase cathepsin D activity. These findings are at odds with other work, which has shown, for example, that glycolic acid applications increase desquamation rates in parallel with an increase in cathepsin D activity in the outer SC (Horikoshi *et al.*, 2005). Yet the amounts of glycolic acid applied in the Horikoshi group's study was as high as 50%, and surface pH was drastically reduced (to ≈2); hence, it is possible that accelerated desquamation reflected toxic effects, unrelated consequences of bulk α-hydroacids, and/or suboptimal pH levels. Increased cathepsin D activates transglutaminase-1, stimulating the formation of the cornified envelope (Egberts *et al.*, 2004), suggesting an alternate, important target for this aspartate protease in barrier function. The cysteine protease, cathepsin L2, another enzyme with an acidic pH optimum, is also expressed as a pro-enzyme in the lower layers of the SC, followed by its activation by as-yet unidentified mechanisms in the outer SC layers (Bernard *et al.*, 2003). Thus, acidification alone also might not suffice to activate cathepsin L2. In summary, it is likely that the effects of hyperacidification are largely restricted to changes in the activities of the relevant lipid-processing and desquamatory SP within the SC, as the activities of desquamatory enzymes with an acidic pH do not appear to increase with hyperacidification.

Yet hyperacidification could, in theory, have adverse effects for the barrier should it decrease the activity of another, important lipid-processing enzyme(s), with a neutral-to-alkaline pH optimum, that is, sPLA$_2$. This apparent paradox can be explained by the fact that hyperacidification is a key consequence of FFA generation by sPLA$_2$ activity, thereby improving barrier function, SC integrity/cohesion, and membrane structure (Fluhr *et al.*, 2004b). Thus, exogenous hyperacidification, as used here, likely bypasses the potentially negative consequences of reduced FFA generation that could result from the inhibition of sPLA$_2$. Pertinently, the acidification of ceramide–cholesterol–FFA mixtures *in vitro* further enhances membrane interactions (Bouwsta *et al.*, 2000), which could represent yet another barrier-improving mechanism of hyperacidification.

The topical application of hydroxyl acids in peels or formulation has been widely used for multiple dermatological conditions from photoaging (Van Scott *et al.*, 1996) to the treatment of congenital (Van Scott and Yu, 1974) or acquired hyperkeratosis (Van Scott and Yu, 1989). Ditre *et al.* (1996) applied 25% glycolic, lactic, or citric acid to the forearm for 6 months, which caused an approximate 25% increase in skin thickness (Ditre *et al.*, 1996). Although the studies were carried out on the forearms, the authors concluded that alpha hydroxyl acids application produced a significant reversal of epidermal and dermal markers of photoaging (Ditre *et al.*, 1996). In our studies, we used lower levels of topically applied PHA not only to decrease SC pH but also to maintain its levels within physiological ranges. Rawlings *et al.* (1996) showed that the topical application of either L- or D-lactic acid (4% in aqueous vehicle) improves permeability barrier function in humans together with increased levels of ceramides in the SC (Rawlings *et al.*, 1996). Accordingly, we found that acidification of membrane domains within the lower SC (i.e., FLIM data) increases both β-GlcCer'ase and aSMase activity, which in turn will increase the lipid processing and ceramide content in the SC. Yet both Rawlings *et al.* (1996) and Berardesca *et al.* (1997) also found that the positive effects of either alpha-hydroxyl acids or PHA on epidermal barrier function are not equal for all acids. This could be linked to the differences in the bioavailability of these acids within SC membrane domains or to the effect of salt formation derived from the neutralization of the applied acids. As our main aim in this study is to assess SC acidification alone, we used as control for our studies the neutralized form of the PHA, thus limiting the positive or negative effects of salt formation. In addition, the bioavailability within the deep domains of the SC PHA was verified using FLIM.

In summary, hyperacidification generates a "super-barrier" largely, if not solely, through its impact on the activities of the lipid-processing and desquamatory enzymes. Moreover, the reduction in pH produces neither inflammation nor hyperplasia, nor changes in epidermal lipid synthesis, further evidence that, under these conditions, PHA do not affect the underlying nucleated cell layers.

Materials and Methods

Materials

Male hairless mice (Skh1/Hr), 6- to 8-weeks old, were purchased form Charles River Laboratories (IFFA Credo, Brussels, Belgium) and fed Purina mouse diet and water *ad libitum*. Four to six mice were used for each treatment in the different experiments (total of 12–16 per experiment). Experiment propylene glycol, ethanol, and hydrochloric acid were from Fisher Scientific (Fairlane, NJ), whereas HEPES buffer, GL (pKa = 2.98), and LBA (pKa = 3.2), two PHA, both of which are "generally accepted as safe" (i.e., GRAS) ingredients, were obtained from Sigma Chemicals (Bornem, Belgium). EnzChek Protease Assay Kit (green fluorescence), Amplex Red Sphingomyelinase and resorufin α-ᴅ-glucopyranoside, and green fluorescent protease inhibitors (STI and pepstatin A) were purchased from Invitrogen (Merelbeke, Belgium). D-Squame-100 tapes of 22 mm were purchased from CuDerm (Dallas, TX). Bradford protein assay kits (Bio-Rad Protein Assay Dye), as well as lyophilized bovine plasma gamma globulin, were purchased from Bio-Rad (Nazareth-Eke, Belgium). All procedures were performed, while mice were anesthetized with chloral hydrate, under protocols approved by the animal care committees of the VAMC (San Francisco; the Universitair Ziekenhuis-Vrije Universiteit Brussels). Hilltop chambers of 25 mm were purchased from Hilltop Research (Miamiville, OH). Antibodies against klk5 and cathepsin D were purchased from Abcam (Cambridge, UK), whereas the anti-klk7 antibodies were a generous gift from Biovitrium (Göteborg, Sweden). Antibodies against DSG1 and DSG3 were purchased from Santa Cruz Biotechnology (Tebu-Bio nv, Boechout, Belgium) and Invitrogen (Zymed).

Acidification protocols

Normal hairless mice were treated twice daily with a single topical application of either LBA or GL (10% (vol/vol), pH 2.8 and 3.2) in PG/E (7:3 (vol/vol)) to 7–8 cm^2 areas on the animals' flanks. Controls were treated similarly with NaOH-neutralized-LBA or -GL (nLBA, nGL) in the PG/E vehicle or vehicle alone. Surface pH was measured with a glass surface electrode, as described above. Skin surface pH was evaluated immediately before and after applications, as well as at 1, 2–3, 6–8, 12, and 20, or 24 hours after applications.

Assessment of pH distribution by FLIM

Freshly excised mouse skin samples were obtained at various points after LBA or vehicle treatment, using the fluorescent pH indicator, BCECF (Invitrogen). BCECF (1 mg of BCECF dissolved in phosphate-buffered saline, then diluted in 70% ethanol to 500 μl) was applied to the treated area four times at 30-minute intervals for 2 hours, before 20 mm^2 punch biopsies were obtained and analyzed by two-photon FLIM. FLIM was used to measure and localize intracellular and extracellular pH throughout the SC (Behne *et al.*, 2002; Hanson *et al.*, 2002). A Millenia-pumped Tsunami titanium:sapphire laser system (Spectra-Physics, Mountain View, CA) was used as the two-photon excitation source, and a two-photon excitation of the sample (<1 mW) was achieved by coupling the 800-nm output of the laser through the epifluorescence port of a Zeiss LSM microscope (Thornwood, NY). The excitation beam was diverted to the sample by a dichroic filter, and the fluorescence was collected using a Hamamatsu (H7422, Bridgewater, NJ) photomultiplier. Scanning mirrors and a ×63 infinity-corrected oil objective (Zeiss F Fluar, 1.3 NA) were used to image areas of 86 μm^2. Z-slices

(2–2.5 μm per slice) were obtained by adjusting the objective focus using a motorized driver (ASI Multi-Scan 4, Lexington, KY). Lifetime data were acquired using the single-photon counting method. Data evaluation and visualization were carried out directly using image analysis software ImageJ (http://rsbweb.nih.gov/ij/index.html). Lower lifetime values represent a more acidic pH. Lifetime values were calibrated to pH values using a calibration curve constructed with pH buffers from pH 4 to 10.

Assessment of epidermal functions

Permeability barrier recovery—To assess the permeability barrier function, TEWL was measured under basal conditions, that is, before acute barrier disruption by repeated Cellophane tape stripping of the flanks of hairless mice (>25 mg cm^{-2} hour^{-1}) using a Tewameter (Courage and Khazaka, Cologne, Germany). Acute disruption was followed by immediate applications of LBA, nLBA, GL, or nGL, as above. Barrier recovery kinetics was assessed 3 hours after PHA or vehicle applications.

SC integrity—To assess changes in SC integrity (i.e., resistance to repeated stripping) in murine skin, sequential D-Squame tape strippings in hairless mice were carried out by a single observer on the flanks of hairless mice 3 hours after the last previous application of LBA, GL nLBA, or nGL. TEWL was evaluated after each tape stripping, with the rate of change in TEWL again compromising SC integrity.

SC cohesion—The amount of protein removed per D-Squame strip defines SC cohesion, as described previously (Dreher *et al.*, 1998). This microassay system was linear in the range of 1–10 μg ml^{-1}, using either human SC from the heel callus or bovine plasma γ-globulin as the protein source (calculated slope $R_f = 0.0297 \pm 0.0006$; Spearman's coefficient: 0.999; $P<0.0001$). Protein content per stripping was then determined using the Bio-Rad Protein Assay Kit, with lyophilized, bovine γ-globulin as the standard in all assays. Each tape was incubated in 1 ml of 1 M NaOH for 1 hour at 37 °C in an incubator shaker at 80 r.p.m., and neutralized thereafter by the addition of 1 ml of 1 M HCl to the scintillation vials. Subsequently, 0.2 ml of this solution was mixed in 0.6 ml distilled water and 0.2 ml of the Bio-Rad protein dye for 5 minutes in borosilicate tubes. After incubations, the reagents were transferred to polystyrene cuvettes, and absorption was measured using a Genesys 5 spectrophotometer (Spectronic, Rochester, NY) at 595 nm. An empty D-Squame tape, as well as distilled water incubated with the Bio-Rad dye, served as negative controls. The amount of calculated protein was then normalized to the skin surface area (μg per cm^2). The amount of removed protein per D-Squame strip corresponded with previous reports of protein removed from untreated skin of hairless mice (i.e., range 2.5–4 μg per strip) (Dreher *et al.*, 1998).

Enzyme activities by *in situ* zymography

SP—Frozen sections (8 μm) from treated hairless mice were rinsed with a washing solution (1% Tween 20 in deionized water) and incubated for 2 hours with 250 μl of BODIPY-Fl-casein in deionized water (2 μl/ml) at 37 °C. Sections were rinsed with the 1% Tween 20 washing solution, coverslipped, and visualized under a confocal microscope (Leica TCS SP, Heidelberg, Germany) at an excitation wavelength of 485 nm and an emission wavelength of 530 nm (Dreher *et al.*, 1998).

β-GlcCer'ase—Frozen sections (8 μm) from treated hairless mice were washed with the 1% Tween 20 washing solution and incubated for 2 hours with 250 μl of 1 mM resorufin α-D-glucopyranoside in deionized water at 37 °C. Sections were rinsed with the washing solution, coverslipped, and visualized under the confocal microscope at an excitation wavelength of 588 nm and an emission wavelength of 644 nm.

aSMase—Frozen sections (8 μm) from treated hairless mice were washed with the 1% Tween 20 washing solution and incubated for 2 hours with 250 μl of 100 m$_M$ Amplex Red reagent (containing 2 U ml^{-1} horseradish peroxidase, 0.2 U ml^{-1} choline oxidase, 8 U ml^{-1} of alkaline phosphatase) in deionized water at 37 °C. Sections were then rinsed with the washing solution, coverslipped, and visualized under the confocal microscope at an excitation wavelength of 588 nm and an emission wavelength of 644 nm.

Protease inhibitor binding assay—Frozen sections (8 μm) from treated hairless mice were washed with the 1% Tween 20 washing solution and incubated for 2 hours with either fluorescent STI (an SPI inhibitor, 1 μg ml^{-1}) or pepstatin A (cathepsin inhibitor, 1 μg ml^{-1}) for 2 and hours at 37 °C. Sections were rinsed with the 1% Tween 20 washing solution, mounted, and visualized under a confocal microscope (Leica TCS SP) at an excitation wavelength of 485 nm and an emission wavelength of 530 nm.

Protein isolation from epidermis

Lipid rafts and non-lipid raft fractions—After skin excision and removal of subcutaneous fat with scalpel blades, samples were floated on 10 m$_M$ dithiothreitol solution in phosphate-buffered saline for 1.5 hours at 37 °C. Subcellular fractions were isolated using ReadyPrep Protein Extraction Kit (Signal and Cytoplasm; Bio-Rad) according to the manufacturer's protocol.

SC extracts—SC was isolated using sequential D-squame tape strippings (20 D-squames per individual; CuDerm). Tapes were then incubated overnight at 4 °C in 1% Triton X-100 and a protease inhibitor cocktail (Complete Mini, Roche, Brussels, Belgium) in phosphate-buffered saline, and then sonicated for 5 minutes at room temperature to extract proteins from the tapes, followed by measurement of the protein content (Bio-Rad Protein Assay Kit).

Western immunoblotting

After protein isolation (see above), the protein content of the whole, basal, and suprabasal epidermal extracts was determined. Equal amounts of protein from each experimental group were loaded onto NuPAGE Novex 10% Bis-Tris Gel (Novex Gel; Invitrogen). After electrophoresis in slab gels, proteins were transferred onto nitrocellulose membranes using the iBlot Dry Blotting System (Invitrogen) and immunoblotted to detect primary antibodies using the Western Breeze Lightening Chemiluminescence Kit (Invitrogen). Western immunoblotting for KLK5 was carried out using the WesternDot 625 Goat Anti-Rabbit Western Blot Kit (Invitrogen) and image detection was carried out using the Image Station 4000MM (Kodak, Raytest, Germany).

Electron microscopy

Biopsy samples were taken from all treatment groups (*n* = 3 animals from each experimental group) and processed for electron microscopy. Samples were minced to <0.5 mm^3, fixed in modified Karnovsky's fixative overnight, and post-fixed in either 0.2% ruthenium tetroxide (RuO$_4$) or 1% aqueous osmium tetroxide (OsO$_4$) containing 1.5% potassium ferrocyanide. After fixation, all samples were dehydrated in graded ethanol solutions, and embedded in an Epon-epoxy mixture. Ultrathin sections were examined, with or without further contrasting with lead citrate, in an electron microscope (Zeiss 10A; Carl Zeiss, Thornwood, NY) operated at 60 kV.

To quantify CD density by electron microscopy, 10 sequential digital images of the outer epidermis were taken at random from each sample, at × 31,500 magnification, for quantitation. The ratio between the total lengths of all CD to the total length of cornified envelopes at the

SG/SC junction, as well as the membrane length surrounding the first SC cell layer, was determined using a planimeter.

Statistical analyses

Statistical analyses were carried out using Prism 2 (GraphPad Software, San Diego, CA). Two groups were compared using Student's *t*-test. Non-parametric Mann–Whitney statistical analyses were carried out to compare percent ratios between different groups of treatments (Morris 2000).

Acknowledgments

References

Behne MJ, Meyer JW, Hanson KM, Barry NP, Murata S, Crumrine D, et al. NHE1 regulates the stratum corneum permeability barrier homeostasis. Microenvironment acidification assessed with fluorescence lifetime imaging. J Biol Chem 2002;277:47399–406. [PubMed: 12221084]

Behrendt H, Green M. Skin pH pattern in the newborn infant. AMA J Dis Child 1958;95:35–41. [PubMed: 13487076]

Berardesca E, Distante F, Vignoli GP, Oresajo C, Green B. Alpha hydroxyacids modulate stratum corneum barrier function. Br J Dermatol 1997;137:934–8. [PubMed: 9470910]

Bernard D, Mehul B, Thomas-Collignon A, Simonetti L, Remy V, Bernard MA, et al. Analysis of proteins with caseinolytic activity in a human stratum corneum extract revealed a yet unidentified cysteine protease and identified the so-called "stratum corneum thiol protease" as cathepsin l2. J Invest Dermatol 2003;120:592–600. [PubMed: 12648222]

Bouwsta JA, Gooris GS, Dubbelaar FE, Ponec M. Phase behaviour of skin barrier model membranes at pH 7.4. Cell Mol Biol (Noisy-le-grand) 2000;46:979–92. [PubMed: 10976878]

Brattsand M, Stefansson K, Lundh C, Haasum Y, Egelrud T. A proteolytic cascade of kallikreins in the stratum corneum. J Invest Dermatol 2005;124:198–203. [PubMed: 15654974]

Caubet C, Jonca N, Brattsand M, Guerrin M, Bernard D, Schmidt R, et al. Degradation of corneodesmosome proteins by two serine proteases of the kallikrein family, SCTE/KLK5/hK5 and SCCE/KLK7/hK7. J Invest Dermatol 2004;122:1235–44. [PubMed: 15140227]

Choi EH, Man MQ, Xu P, Xin S, Liu Z, Crumrine DA, et al. Stratum corneum acidification is impaired in moderately aged human and murine skin. J Invest Dermatol 2007;127:2847–56. [PubMed: 17554364]

Demerjian M, Hachem JP, Tschachler E, Denecker G, Declercq W, Vandenabeele P, et al. Acute modulations in permeability barrier function regulate epidermal cornification: role of caspase-14 and the protease-activated receptor type 2. Am J Pathol 2008;172:86–97. [PubMed: 18156206]

Denda M, Kitamura K, Elias PM, Feingold KR. *trans*-4-(Aminomethyl)-cyclohexane carboxylic acid (T-AMCHA), an anti-fibrinolytic agent, accelerates barrier recovery and prevents the epidermal hyperplasia induced by epidermal injury in hairless mice and humans. J Invest Dermatol 1997;109:84–90. [PubMed: 9204960]

Deraison C, Bonnart C, Lopez F, Besson C, Robinson R, Jayakumar A, et al. LEKTI fragments specifically inhibit KLK5, KLK7, and KLK14 and control desquamation through a pH-dependent interaction. Mol Biol Cell 2007;18:3607–19. [PubMed: 17596512]

Ditre CM, Griffin TD, Murphy GF, Sueki H, Telegan B, Johnson WC, et al. Effects of alpha-hydroxy acids on photoaged skin: a pilot clinical, histologic, and ultrastructural study. J Am Acad Dermatol 1996;34:187–95. [PubMed: 8642081]

Dreher F, Arens A, Hostynek JJ, Mudumba S, Ademola J, Maibach HI. Colorimetric method for quantifying human stratum corneum removed by adhesive-tape stripping. Acta Derm Venereol 1998;78:186–9. [PubMed: 9602223]

Egberts F, Heinrich M, Jensen JM, Winoto-Morbach S, Pfeiffer S, Wickel M, et al. Cathepsin D is involved in the regulation of transglutaminase 1 and epidermal differentiation. J Cell Sci 2004;117:2295–307. [PubMed: 15126630]

Emami N, Diamandis EP. Human kallikrein-related peptidase 14 (KLK14) is a new activator component of the KLK proteolytic cascade. Possible function in seminal plasma and skin. J Biol Chem 2008;283:3031–41. [PubMed: 18056261]

Fartasch M, Teal J, Menon GK. Mode of action of glycolic acid on human stratum corneum: ultrastructural and functional evaluation of the epidermal barrier. Arch Dermatol Res 1997;289:404–9. [PubMed: 9248619]

Fluhr JW, Behne MJ, Brown BE, Moskowitz DG, Selden C, Mao-Qiang M, et al. Stratum corneum acidification in neonatal skin: secretory phospholipase A2 and the sodium/hydrogen antiporter-1 acidify neonatal rat stratum corneum. J Invest Dermatol 2004a;122:320–9. [PubMed: 15009712]

Fluhr JW, Kao J, Jain M, Ahn SK, Feingold KR, Elias PM. Generation of free fatty acids from phospholipids regulates stratum corneum acidification and integrity. J Invest Dermatol 2001;117:44–51. [PubMed: 11442748]

Fluhr JW, Mao-Qiang M, Brown BE, Hachem JP, Moskowitz DG, Demerjian M, et al. Functional consequences of a neutral pH in neonatal rat stratum corneum. J Invest Dermatol 2004b;123:140–51. [PubMed: 15191554]

Giusti F, Martella A, Bertoni L, Seidenari S. Skin barrier, hydration, and pH of the skin of infants under 2 years of age. Pediatr Dermatol 2001;18:93–6. [PubMed: 11358544]

Grubauer G, Elias PM, Feingold KR. Transepidermal water loss: the signal for recovery of barrier structure and function. J Lipid Res 1989;30:323–33. [PubMed: 2723540]

Hachem JP, Behne M, Aronchik I, Demerjian M, Feingold KR, Elias PM, et al. Extracellular pH controls NHE1 expression in epidermis and keratinocytes: implications for barrier repair. J Invest Dermatol 2005a;125:790–7. [PubMed: 16185280]

Hachem JP, Crumrine D, Fluhr J, Brown BE, Feingold KR, Elias PM. pH directly regulates epidermal permeability barrier homeostasis, and stratum corneum integrity/cohesion. J Invest Dermatol 2003;121:345–53. [PubMed: 12880427]

Hachem JP, Houben E, Crumrine D, Man MQ, Schurer N, Roelandt T, et al. Serine protease signaling of epidermal permeability barrier homeostasis. J Invest Dermatol 2006a;126:2074–86. [PubMed: 16691196]

Hachem JP, Man MQ, Crumrine D, Uchida Y, Brown BE, Rogiers V, et al. Sustained serine proteases activity by prolonged increase in pH leads to degradation of lipid processing enzymes and profound alterations of barrier function and stratum corneum integrity. J Invest Dermatol 2005b;125:510–20. [PubMed: 16117792]

Hachem JP, Wagberg F, Schmuth M, Crumrine D, Lissens W, Jayakumar A, et al. Serine protease activity and residual LEKTI expression determine phenotype in Netherton syndrome. J Invest Dermatol 2006b;126:1609–21. [PubMed: 16601670]

Hanson KM, Behne MJ, Barry NP, Mauro TM, Gratton E, Clegg RM. Two-photon fluorescence lifetime imaging of the skin stratum corneum pH gradient. Biophys J 2002;83:1682–90. [PubMed: 12202391]

Holleran WM, Feingold KR, Man MQ, Gao WN, Lee JM, Elias PM. Regulation of epidermal sphingolipid synthesis by permeability barrier function. J Lipid Res 1991;32:1151–8. [PubMed: 1940639]

Holleran WM, Takagi Y, Imokawa G, Jackson S, Lee JM, Elias PM. Beta-glucocerebrosidase activity in murine epidermis: characterization and localization in relation to differentiation. J Lipid Res 1992;33:1201–9. [PubMed: 1431599]

Holleran WM, Takagi Y, Menon GK, Jackson SM, Lee JM, Feingold KR, et al. Permeability barrier requirements regulate epidermal beta-glucocerebrosidase. J Lipid Res 1994;35:905–12. [PubMed: 8071612]

Horikoshi T, Matsumoto M, Usuki A, Igarashi S, Hikima R, Uchiwa H, et al. Effects of glycolic acid on desquamation-regulating proteinases in human stratum corneum. Exp Dermatol 2005;14:34–40. [PubMed: 15660917]

Igarashi S, Takizawa T, Yasuda Y, Uchiwa H, Hayashi S, Brysk H, et al. Cathepsin D, but not cathepsin E, degrades desmosomes during epidermal desquamation. Br J Dermatol 2004;151:355–61. [PubMed: 15327542]

Kim TH, Choi EH, Kang YC, Lee SH, Ahn SK. The effects of topical alpha-hydroxyacids on the normal skin barrier of hairless mice. Br J Dermatol 2001;144:267–73. [PubMed: 11251557]

Kishibe M, Bando Y, Terayama R, Namikawa K, Takahashi H, Hashimoto Y, et al. Kallikrein 8 is involved in skin desquamation in cooperation with other kallikreins. J Biol Chem 2007;282:5834–41. [PubMed: 17182622]

Korting HC, Kober M, Mueller M, Braun-Falco O. Influence of repeated washings with soap and synthetic detergents on pH and resident flora of the skin of forehead and forearm. Results of a cross-over trial in health probationers. Acta Derm Venereol 1987;67:41–7. [PubMed: 2436413]

Krien PM, Kermici M. Evidence for the existence of a self-regulated enzymatic process within the human stratum corneum—an unexpected role for urocanic acid. J Invest Dermatol 2000;115:414–20. [PubMed: 10951277]

Mauro T, Holleran WM, Grayson S, Gao WN, Man MQ, Kriehuber E, et al. Barrier recovery is impeded at neutral pH, independent of ionic effects: implications for extracellular lipid processing. Arch Dermatol Res 1998;290:215–22. [PubMed: 9617442]

Menon GK, Feingold KR, Moser AH, Brown BE, Elias PM. *De novo* sterologenesis in the skin. II. Regulation by cutaneous barrier requirements. J Lipid Res 1985;26:418–27. [PubMed: 4009060]

Menon GK, Ghadially R, Williams ML, Elias PM. Lamellar bodies as delivery systems of hydrolytic enzymes: implications for normal and abnormal desquamation. Br J Dermatol 1992;126:337–45. [PubMed: 1571254]

Morris RE. The use of nonparametric statistics in quantitative electron microscopy. J Electron Microsc 2000;49:545–9.

Nylander-Lundqvist E, Egelrud T. Formation of active IL-1 beta from pro-IL-1 beta catalyzed by stratum corneum chymotryptic enzyme *in vitro*. Acta Derm Venereol 1997;77:203–6. [PubMed: 9188871]

Ohman H, Vahlquist A. *In vivo* studies concerning a pH gradient in human stratum corneum and upper epidermis. Acta Derm Venereol 1994;74:375–9. [PubMed: 7817676]

Ohman H, Vahlquist A. The pH gradient over the stratum corneum differs in X-linked recessive and autosomal dominant ichthyosis: a clue to the molecular origin of the "acid skin mantle"? J Invest Dermatol 1998;111:674–7. [PubMed: 9764852]

Proksch E, Feingold KR, Man MQ, Elias PM. Barrier function regulates epidermal DNA synthesis. J Clin Invest 1991;87:1668–73. [PubMed: 2022737]

Rawlings AV, Davies A, Carlomusto M, Pillai S, Zhang K, Kosturko R, et al. Effect of lactic acid isomers on keratinocyte ceramide synthesis, stratum corneum lipid levels and stratum corneum barrier function. Arch Dermatol Res 1996;288:383–90. [PubMed: 8818186]

Schade H, Marchionini A. Der sauremantel der haut. Klin Wochenschr 1928;7:12–4.

Takagi Y, Kriehuber E, Imokawa G, Elias PM, Holleran WM. Beta-glucocerebrosidase activity in mammalian stratum corneum. J Lipid Res 1999;40:861–9. [PubMed: 10224155]

Thune P, Nilsen T, Hanstad IK, Gustavsen T, Lovig Dahl H. The water barrier function of the skin in relation to the water content of stratum corneum, pH and skin lipids. The effect of alkaline soap and syndet on dry skin in elderly, non-atopic patients. Acta Derm Venereol 1988;68:277–83. [PubMed: 2459871]

Vaccaro AM, Muscillo M, Suzuki K. Characterization of human glucosylsphingosine glucosyl hydrolase and comparison with glucosylceramidase. Eur J Biochem 1985;146:315–21. [PubMed: 3967661]

Van Scott EJ, Ditre CM, Yu RJ. Alpha-hydroxyacids in the treatment of signs of photoaging. Clin Dermatol 1996;14:217–26. [PubMed: 9117988]

Van Scott EJ, Yu RJ. Control of keratinization with alpha-hydroxy acids and related compounds. I. Topical treatment of ichthyotic disorders. Arch Dermatol 1974;110:586–90. [PubMed: 4412623]

Van Scott EJ, Yu RJ. Alpha hydroxy acids: procedures for use in clinical practice. Cutis 1989;43:222–8. [PubMed: 2523288]

Abbreviations

aSMase	acidic sphingomyelinase
BCECF	2,7-bis-(2-carboxyethyl)-5-(and -6)-carboxyfluorescein
β-GlcCer'ase	β-glucocerebrosidase
CD	corneodesmosomes
DSG	desmoglein
FFA	free fatty acid
FLIM	fluorescent lifetime imaging microscopy
GL	gluconolactone
HEPES	4-(2-hydroxyethyl)-piperazine-1-ethanesulfonic acid
klk	kallikrein
LB	lamellar body
LBA	lactobionic acid
LR	lipid raft
nLBA	neutralized LBA
NHE	sodium–proton exchanger
PG/E	propylene glycol/ethanol
PHA	polyhydroxy acids
SC	stratum corneum
SG	stratum granulosum
SP	serine protease
sPLA$_2$	secretory phospholipase A$_2$
STI	soybean trypsin inhibitor
TEWL	transepidermal water loss
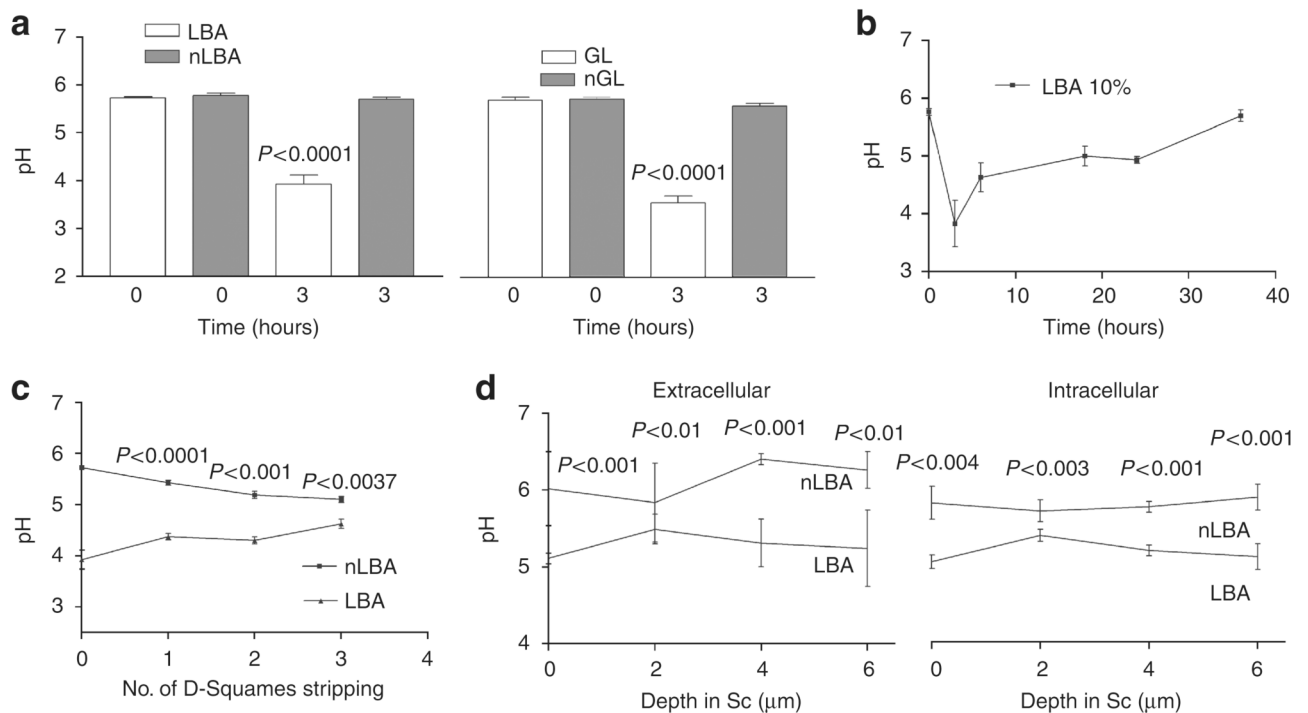
Figure 1. Polyhydroxyl acids (PHA) produce a sustained decrease in SC pH at all levels of the murine stratum corneum
Either lactobionic acid (LBA) and gluconolactone (GL) 10% was applied on murine flanks. (**a**) The decrease in surface SC pH is significant at 3 hours after PHA application in comparison with neutralized (n)-LBA and nGL. (**b**) Surface pH recovers between 16 and 35 hours post single application of LBA. (**c**) LBA-induced acidification extends deep into the SC after application of LBA as shown by the surface pH measurement after sequential tape stripping. (**d**) Similarly, FLIM measurements show that LBA treatment decreased pH within both the cytosolic (intracellular: IC) and membrane microdomains (extracellular: EC) at all levels of murine SC (by about 0.5 pH unit). LBA further acidified membrane microdomains in the lower SC (by about 1 pH unit), extending downward to the SG–SC interface. Results shown in as the mean ± SEM ($n = 4–6$).
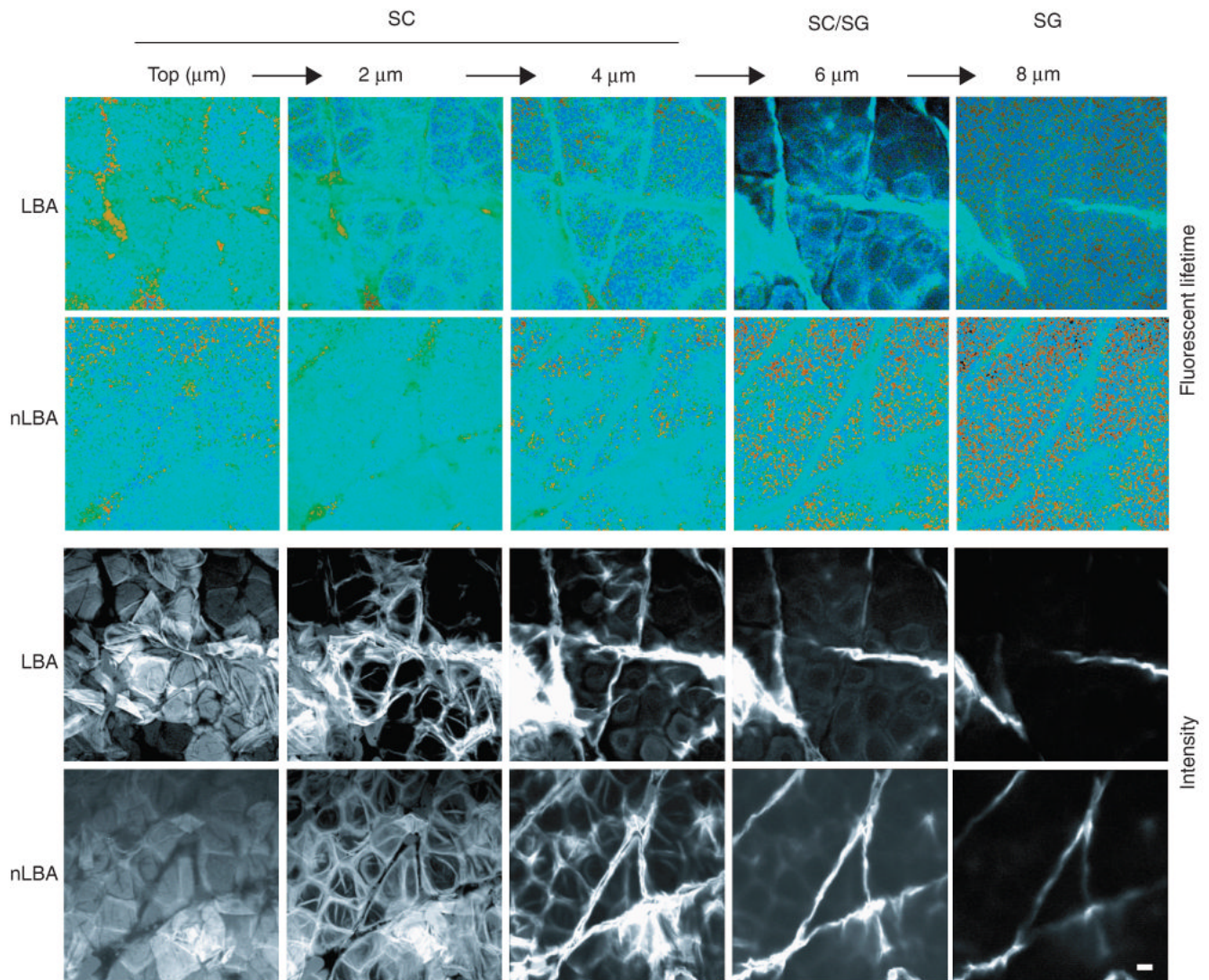
Figure 2. FLIM imaging

Fluorescence Lifetime Imaging (FLIM) of unperturbed stratum corneum treated with LBA vs normalized LBA (nLBA), used as a control. A series of five optical sections is shown, starting at the skin surface (top) and extending to the SG (8 μm). Images are shown en face, and pH is measured by assessing the lifetime of the pH-sensitive moderator BCECF. Intensity imagines (lower two rows) are compared with lifetime images (upper two rows). Light blue represents more neutral values, whereas green and yellow represent more acidic values. Amorphous acidic collections are seen on the surface of the LBA but not on the nLBA-treated skin, likely corresponding to topically applied LBA. Owing to LBA, extracellular acidity is more visible in the LBA-treated SC, although acidification diminishes at the SG, likely representing decreased LBA diffusion at deeper SC/SG levels. Bar = 10 μm.
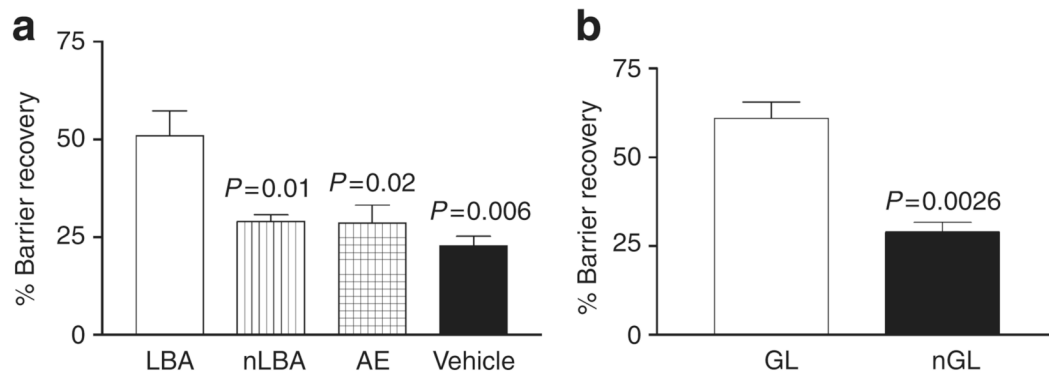
Figure 3. Hyperacidification accelerates barrier recovery in murine skin
TEWL was measured before and at 0, 3, 24, and 48 hours after acute barrier disruption by repeated Cellophane tape stripping on hairless mouse flanks. Similarly, single application of either LBA (**a**) or GL (**b**) 10% immediately after tape stripping to hairless mouse flanks significantly accelerated barrier recovery kinetics 3 hours after disruption in comparison with nLBA, air exposed (AE), V, or nGL. Results shown in as the mean ± SEM (*n* = 4–6).
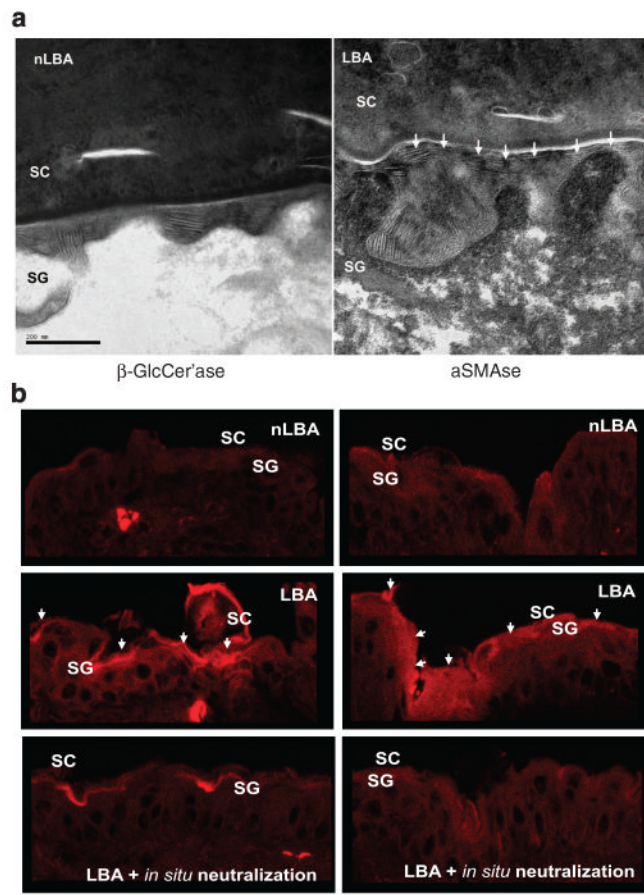
Figure 4. Hyperacidification-induced acceleration in barrier recovery is attributable to accelerated lamellar membrane maturation consequent to β-GlcCer'ase and aSMase activities
(**a**) LBA application immediately after tape stripping of normal murine skin, accelerated processing of lamellar bilayers at the stratum corneum–stratum granulosum (SC–SG) interface (shown by white arrowheads on LBA-treated sites in right panel) in comparison with nLBA-treated (left panel) 3 hours after acute barrier disruption. RuO_4 post-fixation. Bar = 200 nm.
(**b**) Accelerated maturation of lamellar bilayers to an increased *in situ* activity of β-GlcCer'ase and aSMase in outer SG/inner SC interface 3 hours after acute barrier disruption in comparison with nLBA treatment. The increase in β-GlcCer'ase and aSMase activities is pH-dependent and not consequent on an increase in enzyme mass, as *in situ* neutralization downregulates activities of both enzymes to the initial basal level.
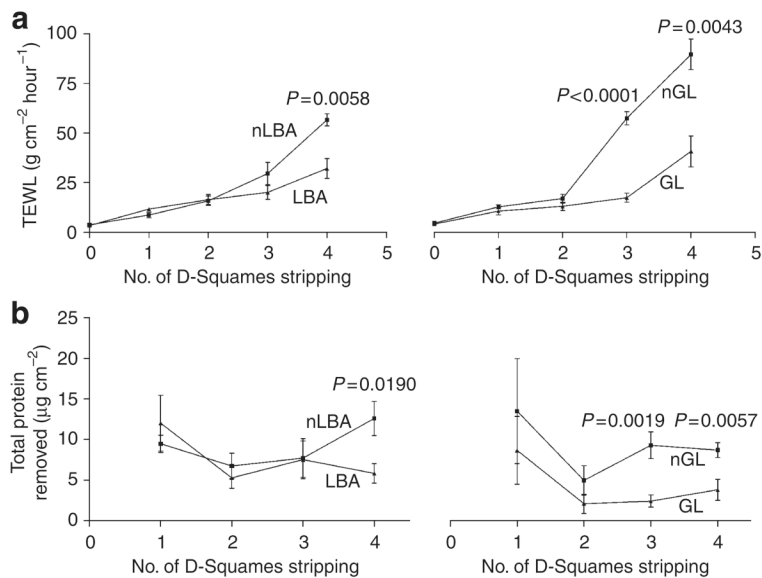
Figure 5. Pre-acidification improves SC integrity/cohesion
To assess the effects of skin acidification on SC integrity/cohesion, LBA and GL were applied to hairless mice flanks. Integrity (**a**) markedly improved in the lower SC 3 hours after a single application of LBA and GL. Similarly, a 3-hour exposure of normal skin to either LBA or GL significantly improved SC cohesion (**b**), again at the lower levels of the SC. Results shown as the mean ± SEM.
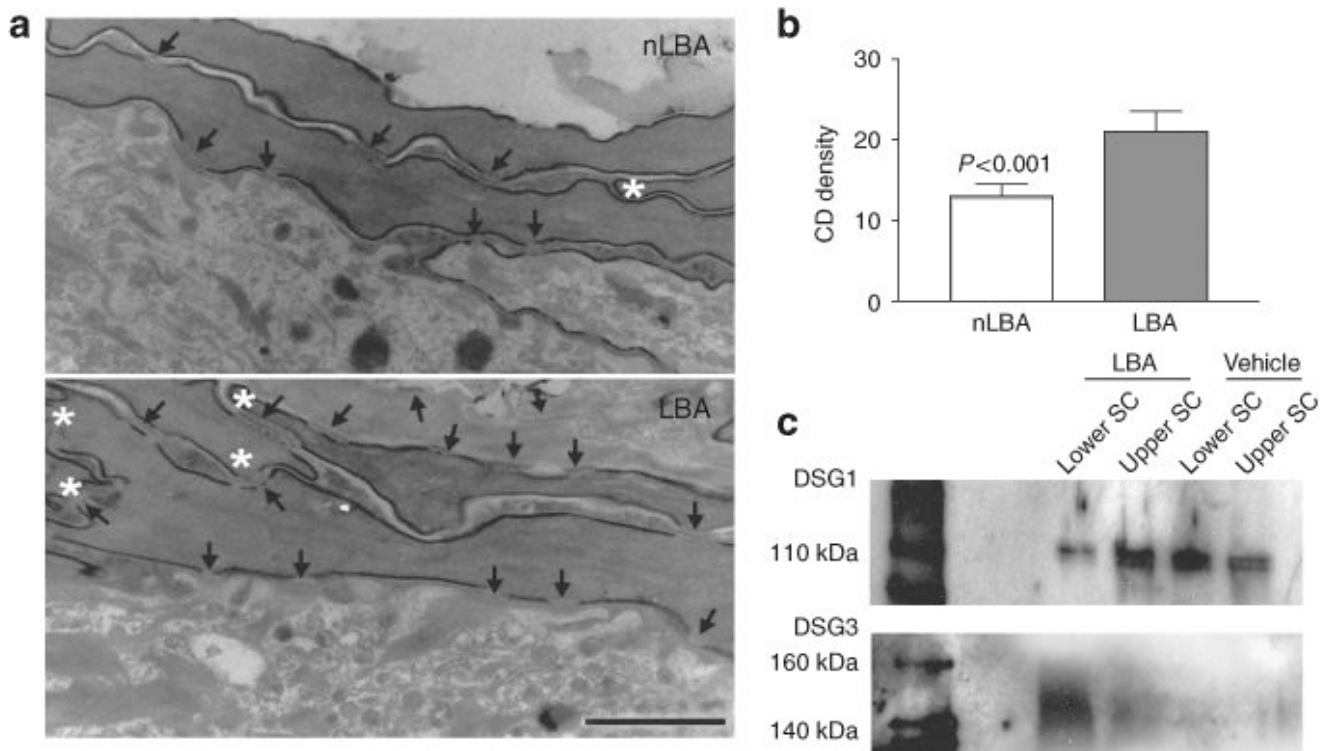
Figure 6. Corneodesmosome (CD) density is increased following acute SC acidification
(**a**) Quantitative EM analysis shows a significant increase in CD density on LBA-treated skin
sites compared with nLBA treatment. (**b**) The number of CD (arrows) is increased and the
lower SC appears more compacted in LBA-treated sites shown by the increased number of
inter-corneocyte hooks (asterisks). Bar = 0.25 μm. (**c**) Western immunoblotting for DSG1 is
reduced in the lower SC in LBA-treated mice compared with vehicle treatment, whereas upper
SC DSG1 are relatively protected from degradations. Yet induction of DSG3 expression is
observed in LBA-treated animals (V = vehicle: propylene glycol: ethanol).
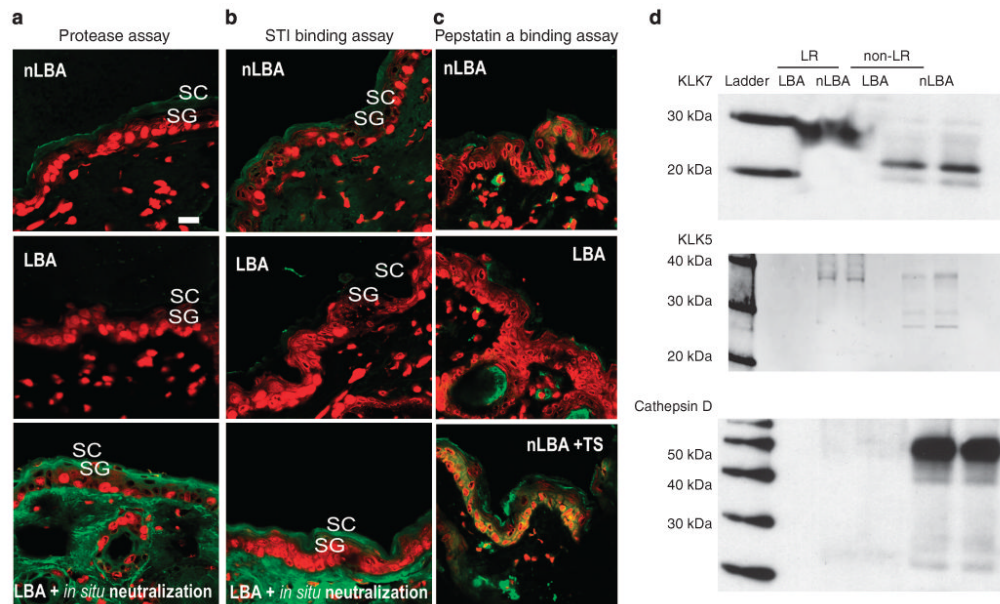
Figure 7. Exposure of normal skin to acid pH is followed by a decrease in basal serine protease (SP) activity and kallikrein (klk) 5 and 7 activation

(**a** and **b**) *In situ* zymography for serine protease (SP) and soybean trypsin inhibitor (STI) binding assay 3 hours after PHA treatment shows a decrease in SP activity on SC acidification sites: LBA- vs nLBA-treated sites. The decrease in SP activities is not due to a decrease in enzyme mass as *in situ* neutralization overrides LBA effect by reactivating SP. Yet fluorescent pepstatin A binding assay (**c**) was carried out on sections from LBA, nLBA-treated normal skin or nLBA-treated tape-stripped (TS) skin to assess cathepsin D activity. Unlike barrier abrogation (TS + nLBA), SC acidification alone does suffice to increase enzyme activity, suggesting a secondary trigger besides pH for cathepsin D activation. (**d**) Western immunoblotting for klk7 and 5 shows decreased immunostaining for the active forms for both proteases (23 and 31 kDa, respectively) in the non-lipid raft (LR) fraction. Note the restriction of pro-klk5 and 7 to the LR domains. A similar pattern of pro-cathespin D (52 kDa) expression with a virtually absent active cathepsin D on both LBA- and nLBA-treated sites was found. Unlike klk5 and 7, pro-cathespin D is restricted to non-LR domains.